

Erosional patterns induced by coral reefs in the eastern coast of Brazil

Padrões erosivos induzidos por recifes de coral na costa leste do Brasil

Gerson FERNANDINO¹, Mauricio GONZÁLEZ², Verónica CÁNOVAS², Clemente Augusto Souza TANAJURA³ & Iracema Reimão SILVA⁴

⁽¹⁾ Programa de Pós-Graduação em Geologia - UFBA, Núcleo de Estudos Hidrogeológicos e do Meio Ambiente – NEHMA. Instituto de Geociências, Universidade Federal da Bahia. Rua Barão de Geremoabo, s/n, Campus Federação, CEP: 40170-290, Salvador, Bahia, Brazil. E-mail: gerson.fernandino@yahoo.com.br.

⁽²⁾ Instituto de Hidráulica Ambiental, Universidad de Cantabria. Avda. Isabel Torres, 15, Parque Cinético y Tecnológico de Cantabria, 39011, Santander, Spain. E-mail: mauricio.gonzalez@unican.es, veronica.canovas@unican.es.

⁽³⁾ Departamento de Física da Terra e do Meio Ambiente, Instituto de Física, Universidade Federal da Bahia. Rua Barão de Geremoabo, s/n, Ondina, CEP: 40170-115, Salvador, Bahia, Brazil. E-mail: cast@ufba.br.

⁽⁴⁾ Department of Oceanography, Núcleo de Estudos Hidrogeológicos e do Meio Ambiente – NEHMA. Instituto de Geociências, Universidade Federal da Bahia. Rua Barão de Geremoabo, s/n, Ondina, CEP: 40170-115, Salvador, Bahia, Brazil. E-mail: iracemars@yahoo.com.br.

Resumo. Praias são ambientes altamente dinâmicos que respondem diretamente a mudanças ocorridas no clima de ondas. Essas mudanças podem influenciar problemas existentes de erosão. O objetivo geral do presente estudo foi descrever o clima de ondas na costa de Porto Seguro, costa leste do Brasil, avaliando como condições de ondas médias e mais energéticas podem influenciar a dinâmica costeira local, e inferindo possíveis causas para os focos de erosão observados na área. O sistema de modelagem costeira SMC-Brasil foi aplicado para avaliar ondas médias e mais energéticas que chegam à costa de modo a calcular padrões de correntes costeiras. As direções de ondas mais frequentes foram de ESE e SE. A presença de recifes de coral adjacentes à costa criam zonas de baixa energia de ondas e focos de maior magnitude de ondas ao longo da costa, resultantes de processos de difração. Recifes de coral e afloramentos de *beachrocks* demonstraram ter um importante papel na formação de padrões de correntes, influenciando os focos de erosão observados na área, que se mostraram intensificados durante os meses de outono/inverno austral.

Palavras-chave. erosão costeira, deriva litorânea, ondas, SMC-Brasil, gerenciamento costeiro

Abstract. Beaches are highly dynamic environments that directly respond to changes in wave climate. These changes may influence already existing erosional problems. The general objective of the present study was to describe the wave climate of the coast of Porto Seguro, eastern Brazil, to evaluate how mean and more energetic wave conditions influence local coastal dynamics, inferring possible causes of erosion focuses observed in the area. The Coastal Modelling System SMC-Brasil was used to assess mean and more energetic waves reaching the coast in order to evaluate coastal current patterns. The most frequent wave directions observed were from ESE and SE. The presence of coral reefs adjacent to the coast created zones of low wave energy and focuses of higher wave magnitude along the coast as a result of diffraction. Coral reefs and beachrock outcrops were shown to play an important role in current patterns and greatly influence the erosion focuses observed in the area, which were found to be intensified during austral autumn/winter months.

Keywords. coastal erosion, longshore transport, waves, SMC-Brasil, coastal management

1 Introduction

Beaches are highly dynamic environments that are deeply influenced by variations in energy (waves, winds and tides), material (sediments) and by beach morphology itself. The dynamic balance of coastal geomorphological units is defined through morphological adjustments in response to changes in sea level, sediment supply and ocean wave climate (Adams *et al.*, 2011). However, coastal geomorphology is not only influenced by processes, but also actively influences its own form in a mutual feedback relationship between processes and shape (Masselink & Gehrels, 2014).

An uneven distribution of wave heights along the coast causes longshore sediment transport and, therefore, leads to erosive/accumulative processes (Griggs & Trenhaile, 1997). Thus, beach erosion is directly associated with wave climate. Areas where higher, more energetic waves occur are more susceptible to erosion than areas where smaller waves reach the coast (Bittencourt *et al.*, 2010).

Mori *et al.* (2010) identified that 70% of sandy beaches in the world are currently suffering erosional processes. While erosion may not be considered a coastal hazard in all locations, the risk imposed to urban beaches may be intensified due to the removal of natural wave buffering zones in much of these areas.

This situation is clearly observed along the eastern coast of Brazil, for example. Bittencourt *et al.* (2005) have identified various sectors of the southern coast of the state of Bahia that are already experiencing severe coastal erosion, which threatens roads and private properties, leading to financial loss and trouble to the local population. This situation may at first seem unlikely given the presence of large coral reef patches in the area, which are usually associated with shoreline protection (Elliff & Silva, 2017). However, the presence of these geological structures promotes complex hydrodynamic processes, which should be analyzed at a more detailed scale to allow mitigation of erosion and impacts on the shoreline.

The study of coastal dynamics depends greatly on obtaining information about sea states in a systematic and continuous way. This is particularly true regarding the characterization of waves that reach the shoreline and interact with natural and anthropogenic features along coastal zones (Almeida *et al.*, 2015). Understanding how a beach functions is an important part of both coastal and oceanic studies (Liu & Losada, 2002). These studies can, in turn, support

coastal management strategies for either mitigating or adapting to current and future conditions (Silva *et al.*, 2003).

The lack of wave data with consistent spatial and temporal resolution is a well-known problem in Brazil, as well as in other developing countries, which hampers studies regarding coastal dynamics and vulnerability (CEPAL, 2011; Almeida *et al.*, 2015). The Coastal Modelling System SMC-Brasil (<http://smcbrasil.ihcantabria.com/>) was developed aiming to fill this information gap and allow the elaboration of coastal studies along the entire coast of Brazil. The system was also designed with the intention to serve as a management tool for local agents to propose and evaluate projects that interfere in the shoreline.

In this context, the objective of the present study was to describe the wave climate of the northern coast of Porto Seguro, Bahia, Brazil, using SMC-Brasil, evaluating at the greatest level of detail so far how mean and more energetic wave conditions influence local coastal dynamics in this area, inferring possible causes for the erosional hotspots observed.

2 Area, materials and methods

2.1 Study area

The study area is located within a region known as Costa do Descobrimento, southern state of Bahia, Brazil. The area encompasses the beaches of the northern coast of the municipality of Porto Seguro (Fig. 1), extending from the left margin of the mouth of the Buranhém River (indicated in Fig. 2) up to the tombolo of Coroa Vermelha, at the border with the municipality of Santa Cruz Cabrália.

The southern coast of the State of Bahia presents high geodiversity and is rich in coastal environments, such as coral reefs, mangrove forests and sandy beaches. Coral reef patches are found across the continental shelf adjacent to the studied shoreline, bordering the Coroa Vermelha, Ponta do Mutá and Ponta Grande tombolos, and the municipality of Porto Seguro (Fig. 1 and Fig. 2) (Leão & Kikuchi, 1999).

The municipality of Porto Seguro presents various historical, cultural and natural attractions. However, the erosive characteristic of some of its beaches reduces the sand strip available for recreational activities and has caused destruction to restaurants and tourism-related buildings, thus compromising this important sector of the local economy.

Geologically, the area consists primarily of Neogene sediments (Barreiras Formation) and secondarily of Quaternary sediments (coral reefs, beachrocks, beach and lagoon deposits)

(Dominguez *et al.*, 2002). The beaches of Porto Seguro consist of Quaternary medium-sized sands, with a small percentage of finer grains associated with wetlands and mangrove deposits.

Figura 1. Localização e geologia da área de estudo. A) O detalhe (retângulo) mostra a localização da área de estudo em relação ao país e ao estado da Bahia. A estrela indica a localização da capital do estado da Bahia, Salvador; B) Detalhe da área de interesse (retângulo): costa norte do município de Porto Seguro, Bahia; e C) Detalhamento da geologia da área de estudo. Sedimentos neogênicos (Formação Barreiras) dominam a porção interna, enquanto sedimentos quaternários (recifes de coral, afloramentos de *beachrocks*, e depósitos lagunares) predominam ao longo da costa. Isóbatas demonstram formas irregulares, especialmente próximo aos recifes de coral e feições de fundo (fonte dos dados geológicos: Dominguez, 2000).
Figure 1. Location and geology setting of the study area. A) Detail (rectangle) shows the location of the study area in relation to Brazil and the state of Bahia. The star indicates the location of the capital of the state of Bahia, Salvador; B) Detail of the area of interest (rectangle): the northern coast of the municipality of Porto Seguro, Bahia; and C) Detail of the geology of the study area. Neogene sediments (Barreiras Formation) dominate the inland area while Quaternary sediments (coral reefs, beachrocks, beach and lagoon deposits) predominate along the coast. Isobaths show irregular shapes, especially near coral reefs and bottom features (geology data source: Dominguez, 2000).

The area was subdivided into three sectors in the present study (from south to north): Sector 1 - from the river mouth up to the third reef patch adjacent to the coast; Sector 2 - from the third reef patch adjacent to the coast up to the Ponta Grande tombolo; and Sector 3 - from the Ponta Grande tombolo up to the northern limit of the municipality of Porto Seguro, between the tombolos of Ponta do Mutá and Coroa Vermelha (Fig. 2).

The shorelines of sectors 1 and 2 present relatively straight beaches with waves breaking directly on the shoreface. Reef patches that are either adjacent or even connected to the coast often interrupt these beaches. Minor salients can be observed at the back of these small patches. Sector 3, consists of large constructive features (tombolos) located adjacent to coral reef patches. Although the study by Dominguez *et al.* (2002) was not conducted with high spatial resolution, complex patterns of wave transformation due to refraction and diffraction were

found behind coral reefs near the coast, indicating that they might be associated with some of the erosive patterns observed in the area.

Figura 2. Praias do município de Porto Seguro subdivididas em três setores. Os principais recifes e afloramentos de *beachrocks* estão identificados por nome, enquanto os focos de erosão, identificados por Silva (2004), estão destacados em vermelho. A interpolação da batimetria foi produzida utilizando o SMC-Brasil.

Figure 2. Beaches of the municipality of Porto Seguro subdivided into three sectors. Main reefs and beachrock outcrops are identified by name and erosional hotspots, identified by Silva (2004), are highlighted in red. Seafloor bathymetry interpolation produced with SMC-Brasil.

One of the most severe (and recurrent) erosive hotspots of the study area is located near the border between sectors 2 and 3. The BR-367 road, which belongs to the national highway network, is the only communication between the center of the municipality of Porto Seguro and the districts located along the Ponta Grande tombolo. In this area, the road approaches the shoreline and is constantly damaged by the erosion of the adjacent beach (Ponta Grande beach), especially during austral autumn/winter months (Mar-Apr-May/Jun-Jul-Aug), when more energetic waves from the southeastern quadrant reach the coast (Martin *et al.*, 1998; Bittencourt *et al.*, 2000) (Fig. 3). Thus, a riprap was built to protect this road. However, this structure proved to be clearly inefficient in protecting the shoreline. Evidence of the high periodicity of these erosive events can be easily obtained through reports from the local media showing the damages to the road. The most recent event was reported on 15 May 2017. Consequently, there is no longer a recreational beach in the area, especially during high water conditions. In addition, the presence of the riprap itself and rocks that collapsed from this structure hamper the access to the beach, thus diminishing its recreational appeal.

Figura 3. Detalhe do tómbolo de Ponta Grande e danos causados pela erosão e medida tomadas para combater seus efeitos. A) Localização dos muros de proteção e enrocamentos construídos para tentar minimizar os efeitos da erosão costeira que afeta a rodovia BR-367 (setas) (Fonte: Google Earth); B) Exemplo de estruturas construídas para proteger propriedades privadas; e C)

Danos causados à rodovia BR-367 após uma tempestade em 2016. Note a presença de enrocamento (rochas) colocados anteriormente como medida de proteção contra erosão.

Figure 3. Detail of the Ponta Grande tombolo and damages caused by coastal erosion and actions taken to minimize its effects. A) Location of shoreline protection walls and ripraps built in order to try to minimize the effects of the coastal erosion that affects the BR-367 road (arrows) (Source: Google Earth). B) Examples of structures built to protect a private property; and C) Damage to the BR-367 road after a storm in 2016. Note the presence of a riprap (rocks) previously placed as a protective measure against erosion.

Apart from a riprap built near the road, protective structures are scarce, except in some private properties where walls were built using either concrete or wood. Sand bags were also placed in an attempt to interrupt or minimize erosive effects (see Fig. 3).

In addition to the previously mentioned coral reefs, beachrock outcrops are found in the southernmost region of the study area, with either parallel or sub-parallel orientation to the shoreline and lengths ranging from 0.3 to 5 km (see Fig. 2).

2.2 Wave, sea level and bathymetry data

The wave and sea level data used in the present study originated from the database of SMC-Brasil (Environmental Hydraulics Institute of Universidad de Cantabria – IHCantabria, Spain). This system comprises a reanalysis of global data producing sea states for every hour over the period between 1948 and 2008 (60 years), called the Global Ocean Waves (GOW) database, which allows the description of deep-water waves (Reguero *et al.*, 2012).

The GOW database, in turn, originated the Downscaled Ocean Waves (DOW) database, which is embedded in SMC-Brasil (Camus *et al.*, 2013). Wave propagation is calculated within SMC-Brasil using the OLUCA model, which interacts with the system's Model for Beach Morphodynamics (MOPLA) and models for currents induced by wave-breaking (COPLA) (González *et al.*, 2007; González *et al.*, 2016). Full descriptions of the SMC-Brasil methodologies and data for waves and sea level are presented by González *et al.* (2016) and in SMC-Brasil manuals available online at <<http://smcbrasil.ihcantabria.com/descargas/>>.

The bathymetry data initially used were obtained through the digitalization of nautical charts (chart No. 1205, scale 1: 30,000, Brazilian Navy and National Institute for Waterway Research) already integrated in SMC-Brasil. Additionally, new bathymetry data was included,

with isobaths beginning at 5 m (Dominguez, 2000). The location and contours of coral reefs and beachrocks were manually improved based on satellite images (Google Earth Pro).

As a convention, in the present study, reefs that are not exposed during low spring tides were considered to be located at 0.5 m in depth, while reefs that are exposed in this condition were considered to emerge 0.5 m above the water.

2.3 Selection of representative cases for describing wave and current patterns

A DOW point (coordinates: $x = 565225$ m, $y = 8177387$ m; UTM WGS 1984, Zone 24 L), was chosen in deep waters ($z = 1560$ m) to initially establish general wave climate conditions.

Three coupled grids were then constructed to execute representative cases selected according to these wave climate results (see Tab. 1). However, due to limitations regarding the regionalization of the atmospheric reanalysis data incorporated in SMC-Brasil (e.g. insufficient spatial resolution of local winds) an additional ENE grid was created to propagate waves from the northeastern quadrant. Thus, four grids (ENE, E, SE and SSE) were designed. Each comprised an external grid with spatial resolution of 100×100 m and a nested grid, with spatial resolution of 25×25 m. Eight control points were distributed along the coast in each grid (Fig. 4).

Tabela 1. Regimes de onda médios e mais energéticos produzidos utilizando o SMC-Brasil para a costa de Porto Seguro, Bahia.

Table 1. Mean and more energetic wave regimes produced using SMC-Brasil for the coast of Porto Seguro, Bahia.

Mean cases ($H_s = 1.5$ m, $T_p = 7.8$ s) were attributed to the ENE and E grids and more energetic cases ($H_s = 3.0$ m, $T_p = 9.8$ s) were attributed to the SE and SSE grids. Waves were propagated to the study area through the OLUCA model (SMC-Brasil) based on the interaction of the four grids designed and local bathymetry. In turn, wave-induced coastal currents were calculated using the COPLA model, which calculates currents associated with wave breaking. The tide amplitude attributed for the propagation of these representative cases was 1.5 m and results were produced for a mean tide height.

Figura 4. Malhas de propagação de ondas. A) Malha ENE; B) Malha E; C) Malha SE; e D) Malha SSE. Notar a localização dos pontos de controle (quadrados coloridos) distribuídos ao longo da costa de Porto Seguro.

Figure 4. Wave propagation grids. A) ENE grid; B) E grid; C) SE grid; and D) SSE grid. Note the location of the control points (colored squares) distributed along the coast of Porto Seguro.

3 Results

3.1 Mean and more energetic wave regimes

The combined analysis of wave height and peak period (Fig. 5) showed that the most frequent waves in the area (mean conditions) presented significant wave heights ranging between 1.0 – 1.5 m and wave periods between 6 – 9 s. For more energetic conditions, wave height ranged between 3.0 – 3.5 m and wave periods between 9 – 12 s.

Figura 5. Resultados de altura de onda e período de pico. A) Distribuição combinada de altura de onda (H_s) e período de pico (T_p); e B) Rosa de ondas. A linha branca indica o $H_{s50\%}$ e a linha vermelha indica o H_{s12} .

Figure 5. Wave height and peak period results. A) Combined distribution of wave height (H_s) and wave peak period (T_p); and B) Wave rose. The white line indicates $H_{s50\%}$ and the red line indicates H_{s12} .

Just over 50% of waves in the area originated from ESE, with mean wave height of 1.53 m and mean peak wave period of 7.45 s. Under more energetic weather conditions for the same direction, mean wave height was 3.17 m and mean peak period was 12.32 s. Table 1 shows a comparative summary of mean and more energetic regimens for the four main wave directions. The remaining directions presented very low occurrence probabilities and were not included in the analysis.

3.2 Seasonal and temporal wave regimes

During the austral spring, summer and winter months (roses A, B and D, respectively), waves from ESE predominate (Fig. 6). However, during austral autumn months (rose C) there is a change in predominant wave direction, in which most waves originate from SE.

Figura 6. Regime de ondas sazonal de Porto Seguro. A) Primavera austral; B) Verão austral; C) Outono austral; e D) Inverno austral. SON: setembro, outubro, novembro; DJF: dezembro, janeiro, fevereiro; MAM: março, abril, maio; e JJA: junho, julho, agosto.

Figure 6. Seasonal wave regime for Porto Seguro. A) Austral spring; B) Austral summer; C) Austral autumn; and D) Austral winter. SON: September, October, November; DJF: December, January, February; MAM: March, April, May; and JJA: June, July, August.

According to the generalized extreme values (GEV) presented in figure 7, which shows return period data of waves approaching the studied coast, waves of approximately 3.4 m have a return period of five years. For this same period, waves with approximately $T_p = 11$ s would occur. Waves measuring 3.8 m, with $T_p = 12$ s, should reach the area every 50 years. These results indicate that more energetic waves may reach the coast of Porto Seguro at different time intervals. However, a longer temporal series may be necessary for confirming this sign presented for 50 years.

Figura 7. Características de ondas com diferentes períodos de retorno que atingem a região de estudo. A) Características de altura significativa de ondas extremas (H_s) para diferentes períodos de retorno para o ponto DOW selecionado em águas profundas; e B) Regime de altura significativa de ondas extremas (H_s) e sua relação com o período de pico (T_p), onde μ é o parâmetro de localização, Ψ é a escala do parâmetro e ξ é a forma do parâmetro. GEV é a abreviação usada para valores extremos generalizados.

Figure 7. Characteristics of waves with different return periods that affect the study area. A) Extreme significant wave height (H_s) characteristics for different return periods for the selected DOW point in deep waters; and B) Extreme significant wave height (H_s) regime its relationship with peak period (T_p), where μ is the location parameter, Ψ is the scale parameter, and ξ is the shape parameter. GEV stands for Generalized Extreme Values.

3.3 Wave height and direction

Wave height and direction results are shown in figures 8 and 9. In these figures, representative cases – a mean condition case (ENE waves) and a more energetic case (SSE waves) – were included for discussion. Results referring to E and SE waves are provided as Supplementary Material.

In general, mean waves from ENE and E presented similar orders of magnitude. Waves from these directions reach the shoreline with low energy because of the transformations they undergo in shallow waters due to bathymetry and the presence of natural obstacles such as coral reef patches (Fig.8A and Supplementary Material). More energetic waves (from SE and SSE) also presented similar orders of magnitude, however they reach the coast with more energy, especially in the northern portion of Sector 2, at the tombolo of Ponta Grande, where the most severe erosional hotspot can be observed (Fig. 8B and Supplementary Material)

Reefs in the study site, especially the De Fora Reef (the largest), cast a low wave energy area (shade zone) over the adjacent coast. These shade zones changed according to wave direction and were observed under both mean and more energetic conditions, though more evident during the latter.

Figura 8. Mapa de isolinhas de altura de ondas (representadas em metros em escala de cinza, de acordo com a barra apresentada à direita) para a área de estudo apresentando os resultados para: A) Exemplo de condições médias de ondas (ENE); e B) Exemplo de condições mais energéticas (SSE).

Figure 8: Wave height isoline maps (represented in meters in grey scale, according to the bar presented to the right) for the study area showing results for: A) Example of mean wave conditions (ENE); and B) Example of more energetic (SSE) wave conditions.

The reefs adjacent to the tombolos of Ponta Grande, Ponta do Mutá and Coroa Vermelha (Sector 3), as well as the beachrock outcrop in the southernmost region of Porto Seguro (Sector 1), also produced a shade zone that partly protected adjacent beaches from direct wave action, especially during mean wave conditions. On the other hand, the presence of channels and

openings between and within these reefs allows the entrance of diffracted waves, which reach the coast with higher erosive potential due to the relatively greater depth of their path (Fig. 9).

Figura 9. Raios de incidência de ondas (representadas em metros em escala de cinza, de acordo com a barra apresentada à direita) para a área de estudo para: A) Exemplo de condições médias de onda (ENE); e B) Exemplo de condições mais energéticas de onda (SSE). Notar os padrões de difração causados pelas estruturas recifais.

Figure 9. Wave ray incidence (represented in meters in grey scale, according to the bar presented to the right) for the study area for: A) Example of mean wave conditions (ENE); and B) Example of more energetic wave conditions (SSE). Note diffraction patterns caused by reef structures.

The Ponta Grande reef provided greater shoreline protection from ENE (Fig. 9A) and E waves (Supplementary Material) to the beaches located in the northern portion of the study area (northern area of Sector 2 and the entire Sector 3). This included the southern area of the Ponta Grande tombolo, near the BR-367 road. The diffraction produced by the southernmost extremity of this reef directs waves towards the border between sectors 1 and 2. Therefore, diffraction processes direct waves with higher magnitude southwards, which reach the beach quasi-perpendicularly.

In the case of SE (Supplementary Material) and SSE waves (Fig. 9B), more intense refraction and diffraction was observed associated, mainly, with the De Fora reef, thus allowing waves with higher magnitudes to reach the area between sectors 1 and 2. For these waves, there was a northward migration of protected zones, a complete elimination of the shade zone created by the Ponta Grande reef in the northern portion of Sector 2, and a decrease of these zones along the beaches located behind these reefs. These conditions allowed more energetic waves to reach these areas.

3.4 Currents along the coast of Porto Seguro

Similarly to the wave height and direction results, coastal current results for all four cases (E, ENE, SE, and SSE) were included as Supplementary Material. Figures 10 and 11 were

included presenting the results for E and SE waves in order to illustrate the discussion. More details on current vectors can be seen in the Supplementary Material.

In general, currents produced by mean condition waves from ENE (Supplementary Material) and E (Fig. 10 and Supplementary Material) were relatively weak (below 0.4 m/s), presenting small intensifications in the surrounding areas of coral reefs and beachrock outcrops and also over these structures. For more energetic waves (SE – Fig. 11 and Supplementary Material – and SSE - Supplementary Material), higher current magnitude was observed (up to 0.8 m/s), thus indicating higher erosional potential.

Figura 10. Intensidade e padrões gerais de correntes ao longo da costa de Porto Seguro para ondas de E. A) Detalhe mostrando a intensificação de correntes sobre os recifes de coral (Setor 3); e B) Detalhe mostrando a intensificação de correntes sobre os afloramentos de *beachrock* (Setor 1). Notar convergência de correntes e correntes de retorno nas aberturas entre recifes de coral adjacentes aos tómbolos no Setor 3. Os eixos correspondem às coordenadas UTM.

Figure 10. Current intensity and general patterns along the coast of Porto Seguro for E waves. A) Detail showing current intensification over coral reefs (Sector 3); and B) Detail showing current intensification over beachrock outcrops (Sector 1). Note current convergence and rip currents in the openings between coral reefs adjacent to the tombolos in Sector 3. Axes correspond to UTM coordinates.

There are three smaller reefs connected to the coast between sectors 1 and 2 that subdivided this area current-wise, generating small circulation cells and hampering the transit of currents along the studied coast.

In Sector 1, the frequent presence of coral reefs and beachrock outcrops did not promote a well-defined pattern of currents for this sector. A “snaking” pattern was observed between these structures (Fig. 11), where longshore currents interact with structures and are deflected offshore and then towards the shore again. The currents observed presented low intensity for all four propagated wave directions and an overall weak SW-NE longshore current, with intensifications over reefs and beachrocks. Current convergence cells, usually associated with rip currents, can be observed between the smaller reefs adjacent to the coast and between tombolos, especially associated with waves from SE (see Fig.11 and Supplementary Material).

In addition, weak rip currents and small convergence zones are also observable. Coastal erosion in this area may be the result of the increase in longshore transport induced by the beachrock outcrop located at the river mouth.

In Sector 2, the absence of reefs and/or beachrock outcrops adjacent to the beach allowed a more defined pattern in current direction for all wave directions analyzed. For ENE waves, the main current direction was NE-SW, driven mainly by the diffraction produced by the Ponta Grande Reef. These currents converge with SW-NE currents from Sector 1 near the border between these two sectors. However, as the angle of incidence increases (clockwise) this convergence zone migrates northwards, producing rip currents that may transport sediment offshore.

Finally, in Sector 3, the intensification of currents over reefs and the influence they have on current direction becomes more evident. Currents associated with the tombolos converge and produce rip currents that pass through the channels/openings between and within reefs and move offshore, transporting sediments.

Figura 11. Correntes geradas por ondas de SE. Detalhe mostra um exemplo de padrão “serpenteante” de correntes sobre os pequenos bancos recifais adjacentes à costa de Porto Seguro. Os eixos correspondem às coordenadas UTM.

Figure 11. Currents generated by SE waves. Detail shows an example of a “snaking” current pattern over small reef patches adjacent to the coast of Porto Seguro. Axes correspond to UTM coordinates.

4 Discussion

Other studies have successfully used the SMC-Brasil to evaluate erosion problems in coastal areas from Brazil (Almeida et al., 2015, Silva et al. 2016, Silva et al. 2017). Although also presenting limitations intrinsic to this computational tool, their results were satisfactory and well represented the reality of their respective study areas, as the present study.

Over the past decades, coral reefs have been shown to efficiently decrease wave height and wave energy, effectively reducing coastal hazard risks (i.e. Young, 1989; Ferrario *et al.*, 2014). Bittencourt et al. (2010) also indicated that coral reefs and beachrock outcrops in the

northern coast of the state of Bahia were responsible for wave energy attenuation. However, as indicated by Elliff & Silva (2017), the full array of variables involved in shoreline protection by coral reefs has not been entirely investigated. Reef morphology (i.e. fringing reefs, barrier reefs, reef patches, atolls, etc.) and rugosity combined to local coastal dynamics yields site-specific results. For example, in the case of the Indian Ocean tsunami of 2004, channels between reefs potentially accelerated the water flow and led to greater coastal flooding behind coral reefs, decreasing their efficiency against coastal flooding (UNEP-WCMC, 2006). In the case of the present study, coral reefs did not seem to protect the shoreline as a whole. The results showed that they potentially induced some of the erosional hotspots currently observed, while protecting other portions of the shoreline. Their morphology, size and distance from the shore combined with different wave directions, yielded different responses regarding coastal erosion. In addition, channels between reef patches adjacent to the tombolos seem to favor the erosion observed in these areas.

During the incidence of cold fronts, more energetic SSE waves reach the beaches that were otherwise protected by ENE and E waves. This fact was also observed by other authors for the north coast of the state of Bahia (Dominguez et al. 1992, Martin et al. 1998, Bittencourt et al. 2005). Wave vectors reach the northern portion of the beach in Sector 2 (Ponta Grande) more directly, since the De Fora reef, which is the largest reef structure near the shoreline, does not cast a shade zone in that direction in these conditions. This reef causes wave diffraction, which associated with the diffraction caused by the Itassepanema reef, allows waves to reach this area more directly. This could be one of the reasons for the erosion observed to cause damages to the BR-367 road in the area.

With increasing efforts towards implementing green infrastructure to promote ecosystem services such as shoreline protection, decision-makers and stakeholders should not overlook the dangers of applying “one size fits all” strategies. Knowledge on local processes is imperative to reach the best outcomes for human well-being and for the environment (Ruckelshaus *et al.*, 2015). Thus, coastal modelling systems such as SMC-Brasil, which compiles wave information for data-deficient areas, present high potential to empower local researchers.

Currents were weak and highly influenced by the presence of structures. Convergence cells migrated northwards as the angle of incidence of waves increased. In the area, reefs and beachrock outcrops were responsible for an intensification of currents. This may be the main cause of the erosion observed along Sector 1. The authors highlight the fact that the “snaking”

pattern observed may not entirely represent reality, being the combined result of the bathymetry data interpolation and limitations of the current generating tool in SMC-Brasil in areas shallower than 5 meters.

The morphology of the coast of Porto Seguro, the frequent presence of reef patches of different sizes, positions and distances from the coast, as well as the uncertainties regarding the definition of the bathymetry, grids and reef shapes and depth, did not allow for an observation of a defined current pattern. This hindered the definition of a preferential direction of currents associated with the various wave directions analyzed.

The insufficient spatial resolution of local winds posed some limitation to the use of SMC-Brasil in this case study. While the most frequent wave directions observed were ESE (50.8%) and SE (33.1%), previous regional studies indicated that the most frequent wave directions for the area were E (35%) and NE (31%), while waves from SE and SSE accounted for 21% and 13% of occurrences, respectively (Hogben & Lumb, 1967). More recently, Pianca *et al.* (2010), using NOAA Wave Watch III data, showed that the N and NE wave signal was present during summer and spring, though at very low frequencies (usually below 10%). These authors' results showed predominance of E waves during the summer (41.3%), winter (40.5%), and spring (34.1%). During autumn, S waves predominated (47.3%). The S and SE components were present in relevant frequencies during all seasons. An underrepresentation of waves from the NE quadrant was also observed by Silva *et al.* (2016) and Silva *et al.* (2017).

In order to overcome the system's deficiency, a northeastern wave quadrant case (ENE) was created based on the literature in order to evaluate the local incidence of waves from this direction. Although the wind field may underestimate the incidence of NE waves, the time-averaged results showed fine agreement between modeled and observational data from other studies and the results found in the present study.

Another important aspect regarding potential for coastal erosion and coastal management strategies were the return periods observed in the present study. Waves measuring 3 m in height and with peak periods of approximately 10 s presented a return period of over one year, indicating that their incidence is relevant, frequent, and must be taken into account when considering coastal management and risk reduction. In addition, more energetic events presented return periods of two and five years, thus increasing ongoing erosional processes. This should be taken into account by decision makers when planning interventions in the coastal zone of Porto Seguro, such as the construction of shoreline protection structures.

Coastal erosion fits the definition of hazard proposed by the United Nations International Strategy for Risk Reductions (UNISDR, 2009), considering that this process

represents a condition that may promote injuries, loss of life, damage to property, loss of livelihoods, social and economic disruption, and environmental damage. As such, vulnerable areas should seek strategies to increase their resilience, allowing local communities to recover fully from adverse events.

As shown in the present study, the municipality of Porto Seguro already faces the impacts of coastal erosion, especially in the area of Ponta Grande where part of the BR-367 road has been damaged. Management strategies should be applied in the area and should take into account the particularities of the area in order to be effective in tackling the problem. The construction of underwater breakwaters was suggested by other authors as a possible solution for erosional problems in northeastern Brazil (Mallman & Pereira, 2014). This was specifically suggested due to the fact that these structures simulate coral reefs. However, due to the geomorphology complexity of Porto Seguro, such engineering interventions should be carefully considered before being implemented in order to avoid future problems. The management strategies “accommodate”, “expand into the coastal zone” and “hold the line” proposed by the Wellington City Council Sea Level Rise Option Analysis report (WCC 2013) should be a possible solution for Porto Seguro to cope with an imminent sea-level rise. The first couple of strategies could be used in the case of the recreational complexes (bars and restaurants) found on the shoreline that not only suffer from the consequences of coastal erosion, but also seem to induce them. These structures could be relocated or rebuilt as suspended structures (stilts) to reduce the effects of sea-level rise. In turn, for the BR-367 road, the last couple of strategies could be implemented. Therefore, the road could be either elevated or moved into the coastal zone. In addition to these strategies, the removal of s ripraps, beach nourishment and reforestation of lost areas of dune vegetation should be implemented.

5 Conclusions

Although different (in terms of magnitude and frequency) from the regional results found in the literature, the local wave results of the present study agreed with general patterns found in modeled and observational studies, thus indicating that SMC-Brasil can be successfully applied in Brazilian beaches, especially for management purposes.

The various coral reef structures present adjacent to the coast are responsible for uneven wave energy distribution along the coast by creating low wave energy zones and focuses of higher wave magnitude as a result of wave diffraction.

Waves from SE and SSE seem to be responsible for the most concerning erosion hotspot of the area (sector 2), which is intensified under stormy conditions. Thus, the present study represents an important baseline for local decision makers to effectively respond to the severe erosional problem that constantly damages the most important access road (BR-367) between the center of the municipality and districts located along the tombolos, causing great losses to the local population. Moreover, the present study provides important information about the local dynamics at the most detailed level yet, which may aid future coastal engineering projects designed to solve or mitigate problems caused by coastal erosion.

Acknowledgments. G. Fernandino thanks the *Conselho Nacional de Desenvolvimento Científico e Tecnológico* (CNPq) for his PhD scholarship (Process No. 140817/2014-0) and the Environmental Hydraulics Institute, Universidad de Cantabria, Spain, for providing data and training and for supporting this study. He also thanks Carla Elliff for her valuable insights and discussions from the point of view of ecosystem services that greatly contributed to the present study
M. González and V. Cánovas acknowledge the support of the *Sociedad para el Desarrollo Regional de Cantabria* (SODERCAN) under Grant ID16-IN-045.

References

- Adams, P.N., Inman, D.L. & Lovering, J.L. 2011. Effects of climate change and wave direction on longshore sediment transport patterns in Southern California. *Climate Change*, 109(Suppl. I): S2011-S228.
- Almeida, L.R., Amaro, V.E., Marcelino, A.M.T. & Scudelare, A.C. 2015. Avaliação do clima de ondas da praia de Ponta Negra (RN, Brasil) através do uso do SMC-Brasil e sua contribuição à gestão costeira. *Journal of Integrated Coastal Zone Management*, 15(2): 135-151.
- Bittencourt, A.C.S.P., Dominguez, J.M.L., Martin, L. & Silva, I.R. 2000. Patterns of sediment dispersion coastwise the state of Bahia-Brazil. *Anais da Academia Brasileira de Ciências*, 72(2): 271-287.

- 571 Bittencourt, A.C.S.P., Dominguez, J.M.L., Martin, L. & Silva, I.R. 2005. Longshore transport
572 on the northeastern Brazilian coast and implication to the location of large-scale
573 accumulative and erosive zones: an overview. *Marine Geology*, 219(4): 219-234.
- 574 Bittencourt, A.C.S.P., Livramento, F.C., Dominguez, J.M.L. & Silva, I.R. 2010. Tendência de
575 longo prazo à erosão costeira num cenário perspectivo de ocupação humana: litoral norte
576 do estado da Bahia. *Revista Brasileira de Geociências*, 40(1): 125-137.
- 577 Camus, P., Mendez, F.J., Medina, R., Tomas, A. & Izaguirre, C. 2013. High resolution
578 downscaled ocean waves (DOW) reanalysis in coastal areas. *Coastal Engineering*, 72:
579 56-68.
- 580 Dominguez J.M.L, Bittencourt A.C.S.P. & Martin L. 1992. Controls on Quaternary coastal
581 evolution of the east-northeastern coast of Brazil: roles of sea-level history, trade winds
582 and climate. *Sedimentary Geology*, 80:213-232.
- 583 Dominguez, J.M.L. 2000. *Projeto Costa do Descobrimento: avaliação da potencialidade*
584 *mineral e subsídios ambientais para o desenvolvimento sustentável dos municípios de*
585 *Belmonte, Santa Cruz de Cabralia, Porto Seguro e Prado*. Salvador, CBPM/CPRM –
586 CBPM/UFBa-CPGG/LEC, 163p.
- 587 Dominguez, J.M.L., Martin, L. & Bittencourt, A.C.S.P. 2002. A Costa do Descobrimento, BA:
588 a geologia vista das caravelas. In: Schobbenhaus, C., Campos, D.A., Queiroz, E.T.,
589 Winge, M. & Berbert-Born, M.L.C. (Eds.) *Sítios Geológicos e Paleontológicos do Brasil*.
590 Brasília, DNPM/CPRM/SIGEP, p. 233-241.
- 591 CEPAL (Comisión Económica para América Latina y el Caribe) 2011. *Efectos del cambio*
592 *climático en la costa de América Latina y el Caribe: dinámicas, tendencias y variabilidad*
593 *climática*. NU, CEPAL, 265p.

- 594 Elliff, C.I. & Silva, I.R. 2017. Coral reefs as the first line of defense: Shoreline protection in
595 face of climate change. *Marine Environmental Research*, 127:148-154.
- 596 Ferrario, F., Beck, M.W., Storlazzi, C.D., Micheli, F., Shepard, C.C. & Airoidi, L. 2014. The
597 effectiveness of coral reefs for coastal hazard risk reduction and adaptation. *Nature*
598 *Communications*, 5: 1-9.
- 599 González, M., Medina, R., Gonzalez-Ondina, J., Osorio, A., Méndez, F.J. & García, E. 2007.
600 An integrated coastal modeling system for analyzing beach processes and beach
601 restoration projects, SMC. *Computers & Geosciences*, 33(7): 916-931.
- 602 González, M., Nicolodi, J.L., Gutiérrez, O.Q., Losada, V.C. & Hermosa, A.E. 2016. Brazilian
603 coastal processes: wind, wave climate and sea level. *In*: Short, A.D. & Klein, A.H.F.
604 (Eds.) *Brazilian Beach Systems*. Switzerland, Springer International Publishing, 608p.
- 605 Griggs, G.B. & Trenhaile, A.S. 1997. Coastal cliffs and platforms. *In*: Carter, R.W.G. &
606 Woodroffe, C.D. (Orgs.) *Coastal Evolution-Late Quaternary shoreline*
607 *Morphodynamics*. Cambridge, Cambridge University Press, p. 425-450.
- 608 Hogben, N. & Lumb, F.E. 1967. *Ocean Wave Statistics*. London, HMSO, 263p.
- 609 Leão, Z.M.A.N. & Kikuchi, R.K.P. 1999. The Bahian coral reefs – from 7000 years BP to 2000
610 years AD. *Ciência e Cultura Journal of the Brazilian Association for the Advancement of*
611 *Science*, 51: 262-273.
- 612 Liu, P.L.F. & Losada, I.J. 2002. Wave propagation modeling in coastal engineering. *Journal of*
613 *Hydraulic Research*, 40(3): 229-240.

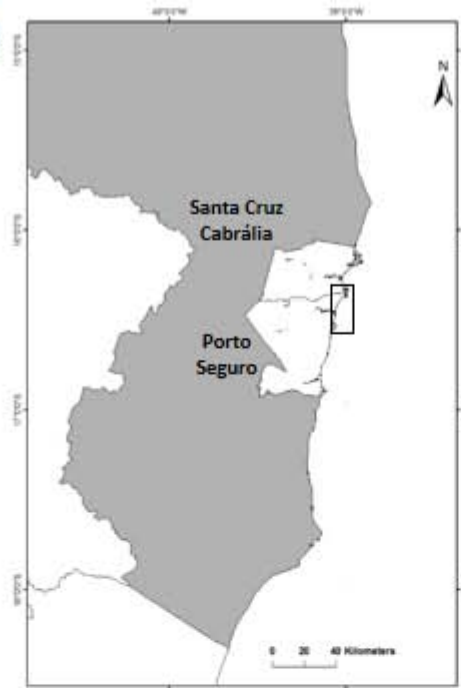
- 614 Mallmann, D.L.N. & Pereira, P.S. 2014. Coastal erosion at Maria Farinha Beach, Pernambuco,
615 Brazil: Possible causes and alternatives for shoreline protection. *Journal of Coastal*
616 *Research*, 71(SI):24-29.
- 617 Martin, L., Dominguez, J.M.L. & Bittencourt, A.C.S.P. 1998. Climatic control of coastal
618 erosion during a sea-level fall episode. *Anais da Academia Brasileira de Ciências*, 70:
619 249-266.
- 620 Masselink, G. & Gehrels, R. 2014. Introduction to coastal environments and global change. *In*:
621 Masselink, G. & Gehrels, R. (Eds.) *Coastal environments & global change*. Chichester,
622 West Sussex, John Wiley & Sons, Ltd, p. 1-25.
- 623 Mori, N., Yasuda, T., Mase, H., Tom, T. & Oku, Y. 2010. Projection of Extreme Wave Climate
624 Change under Global Warming. *Hydrological Research Letters*, 4: 15-19.
- 625 Pianca, C., Mazzini, P.L.F. & Siegle, E. 2010. Brazilian offshore wave climate bases on NWW3
626 reanalysis. *Brazilian Journal of Oceanography*, 58(1): 53-70.
- 627 Reguero, B.G., Menéndez, M., Méndez, F.J., Mínguez, R. & Losada, I.J. 2012. A Global Ocean
628 Wave (GOW) calibrated reanalysis from 1948 onwards. *Coastal Engineering*, 65: 38-55.
- 629 Ruckelshaus, M., McKenzie, E., Tallis, H., Guerry, A., Daily, G., Kareiva, P., Polasky, S.,
630 Ricketts, T., Bhagabati, N., Wood, S.A. & Bernhardt, J. 2015. Notes from the field:
631 lessons learned from using ecosystem service approaches to inform real-world decisions.
632 *Ecological Economics*, 115:11-21.
- 633 Silva, I.R., Bittencourt, A.C.S.P., Dominguez, J.M.L & Silva, S.B.M. 2003. Uma contribuição
634 à gestão ambiental da Costa do Descobrimento (litoral sul do estado da Bahia): Avaliação
635 da qualidade recreacional das praias. *Geografia*, 28(3): 397-413.

- 636 Silva, I.R. (2004). *Costa do Descobrimento: uma contribuição para gestão ambiental*.
 637 Salvador, 232 p. Tese de Doutorado, Programa de Pós-graduação em Geologia, Instituto
 638 de Geociências, Universidade Federal da Bahia.
- 639 Silva, I.R., Guimarães, J.K., Bittencourt, A.C.S.P., Rodrigues, T.K. & Fernadino, G. 2016.
 640 Modelagens de clima de ondas e transporte sedimentar utilizando o SMC-Brasil:
 641 aplicações para a Praia do Forte, litoral norte do estado da Bahia. *Revista Brasileira de*
 642 *Geomorfologia*, 17(4):743-761.
- 643 Silva, I.R., Guimarães, J.K., Bittencourt, A.C.S.P., Rodrigues, T.K. & Fernadino, G. 2017.
 644 Avaliação da dinâmica litorânea da região de Baixo/Barra do Itariri, litoral norte do
 645 Estado da Bahia, utilizando o Sistema de Modelagem Costeira (SMC-Brasil). *Pesquisas*
 646 *em Geociências*, 44(2):221-234.
- 647 UNEP-WCMC (United Nations Environment Programme World Conservation Monitoring
 648 Centre). 2006. *In the front line: shoreline protection and other ecosystem services from*
 649 *mangroves and coral reefs*. Cambridge, UNEP-WCMC, 44p.
- 650 UNISDR (United Nations International Strategy for Risk Reductions). 2009. *Terminology on*
 651 *Disaster Risk Reduction*. Geneva, United Nations, 35p.
- 652 WCC – Wellington City Council. (2013). *Sea Level Rise Options Analysis*. Wellington: Tonkin
 653 & Taylor Ltd.
- 654 Young, I.R. 1989. Wave transformation over coral reefs. *Journal of Geophysical Research*,
 655 94(C7):9779-9789.

A








B




LEGEND


Holocene

-  Clay-organic deposits (wetlands)
-  Clay-organic deposits (mangrove)
-  Beachrock banks
-  Regressive coastal sand deposits (QH)
-  Coral reefs


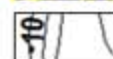
Quaternary

-  Residual sand deposits ("Mussurunga")

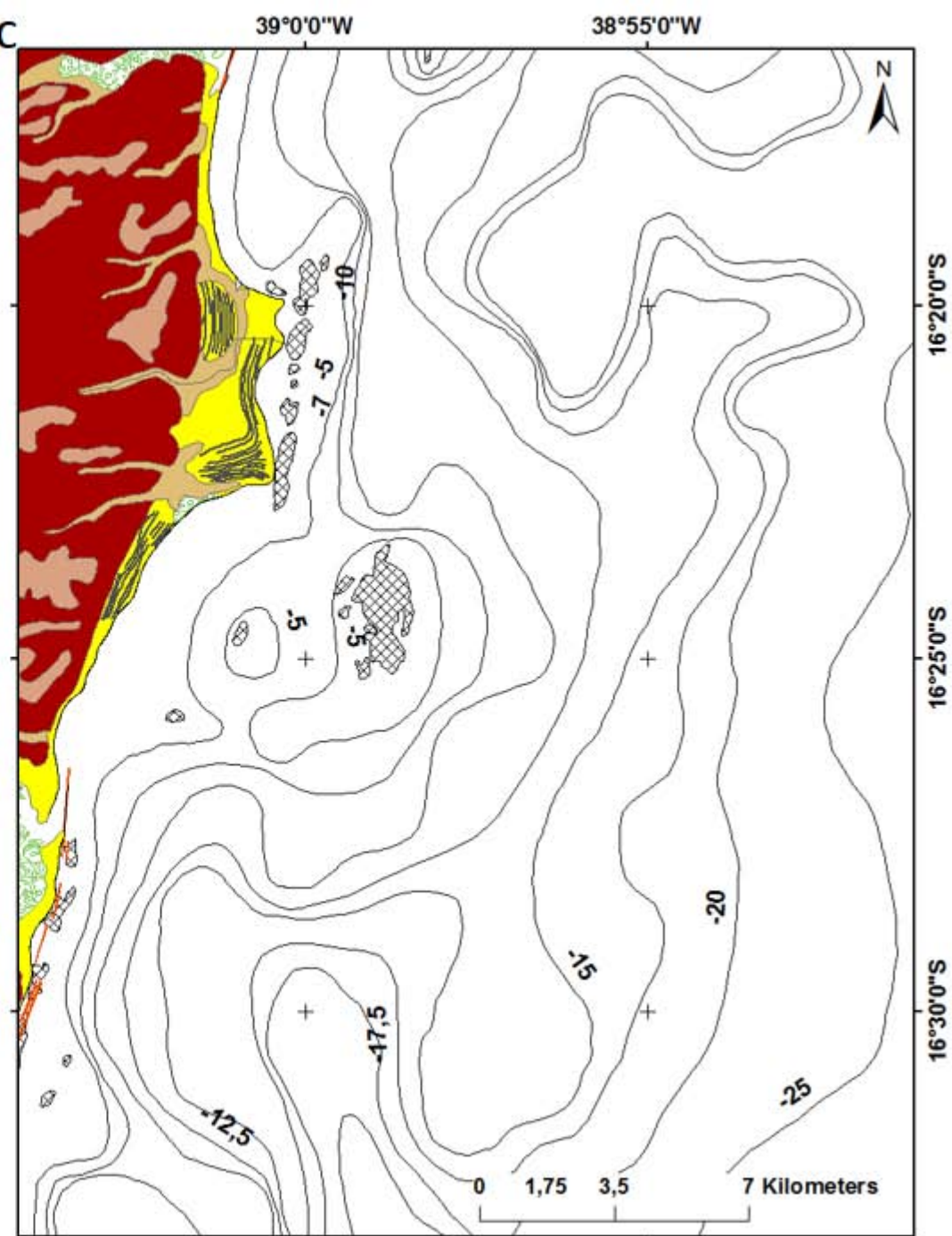
Neogene

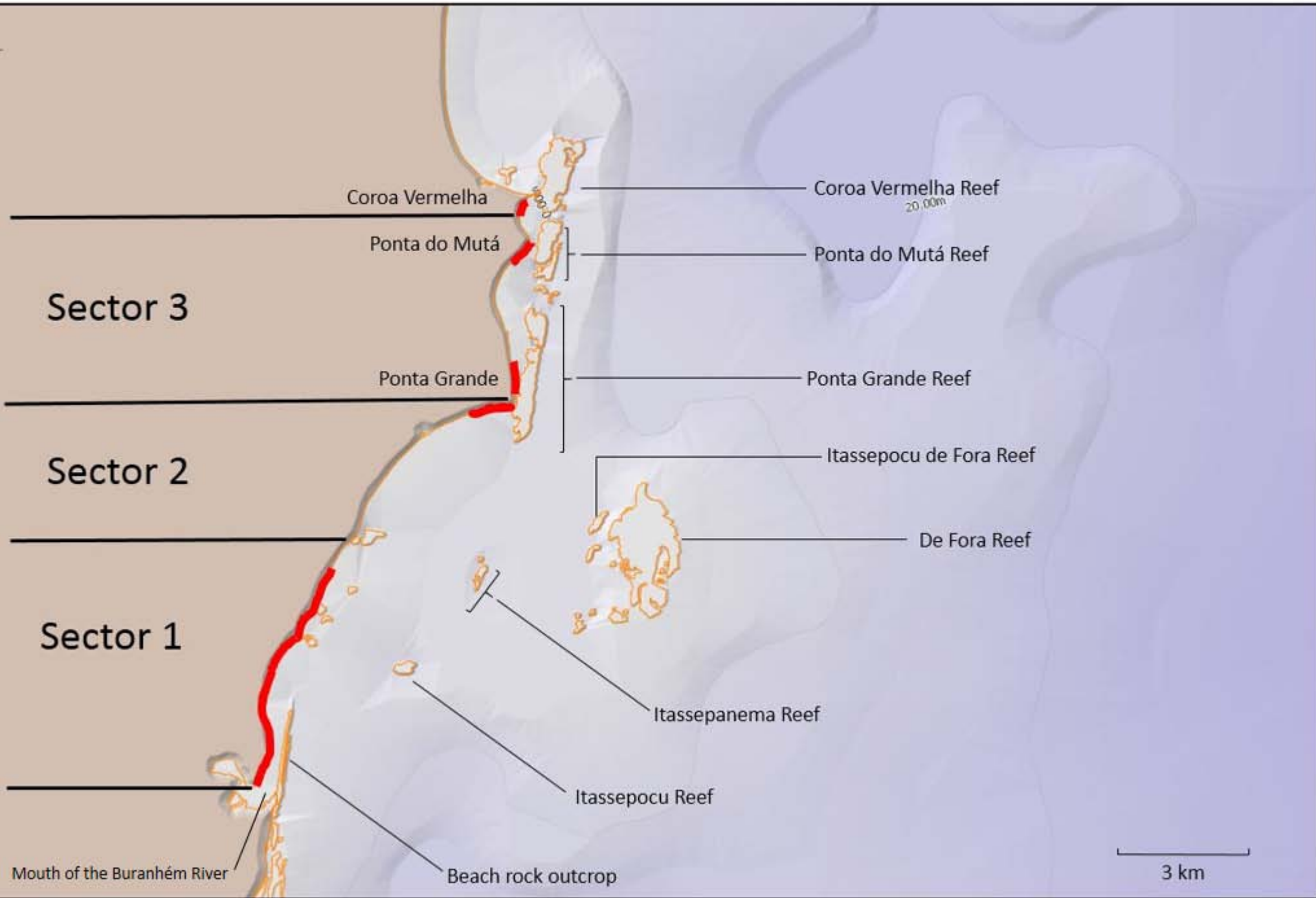
-  Barreiras Group

Geologic conventions

-  Beach ridges
-  Isobaths

C





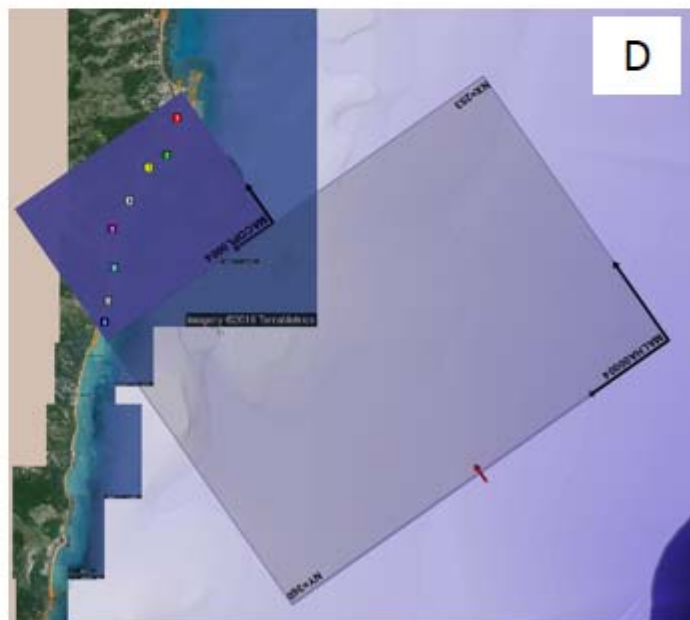
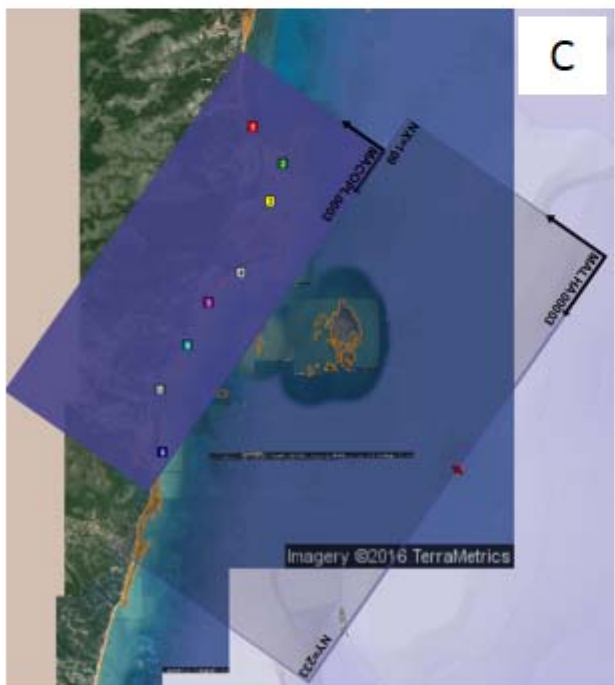
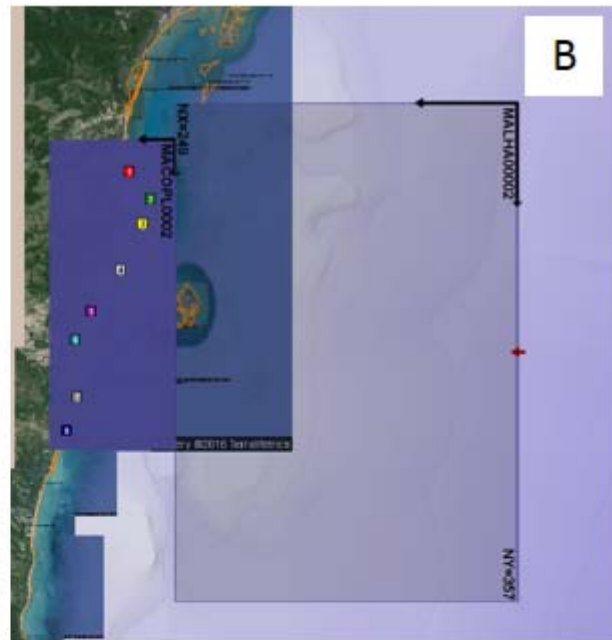
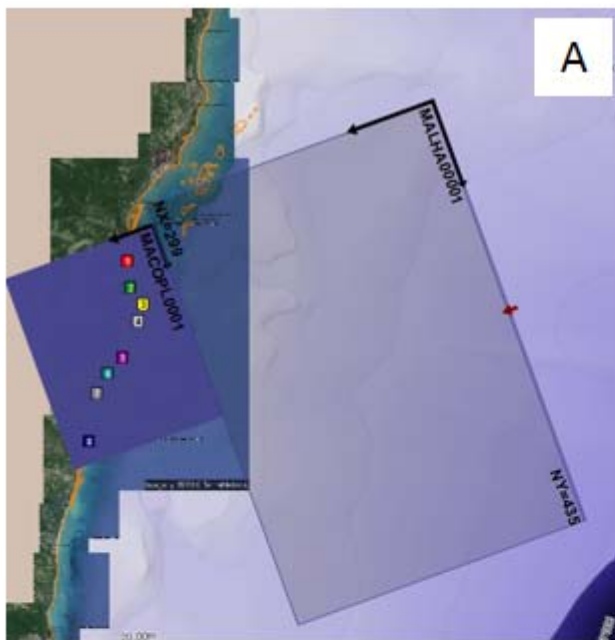
Mouth of the Buranhém River

Beach rock outcrop

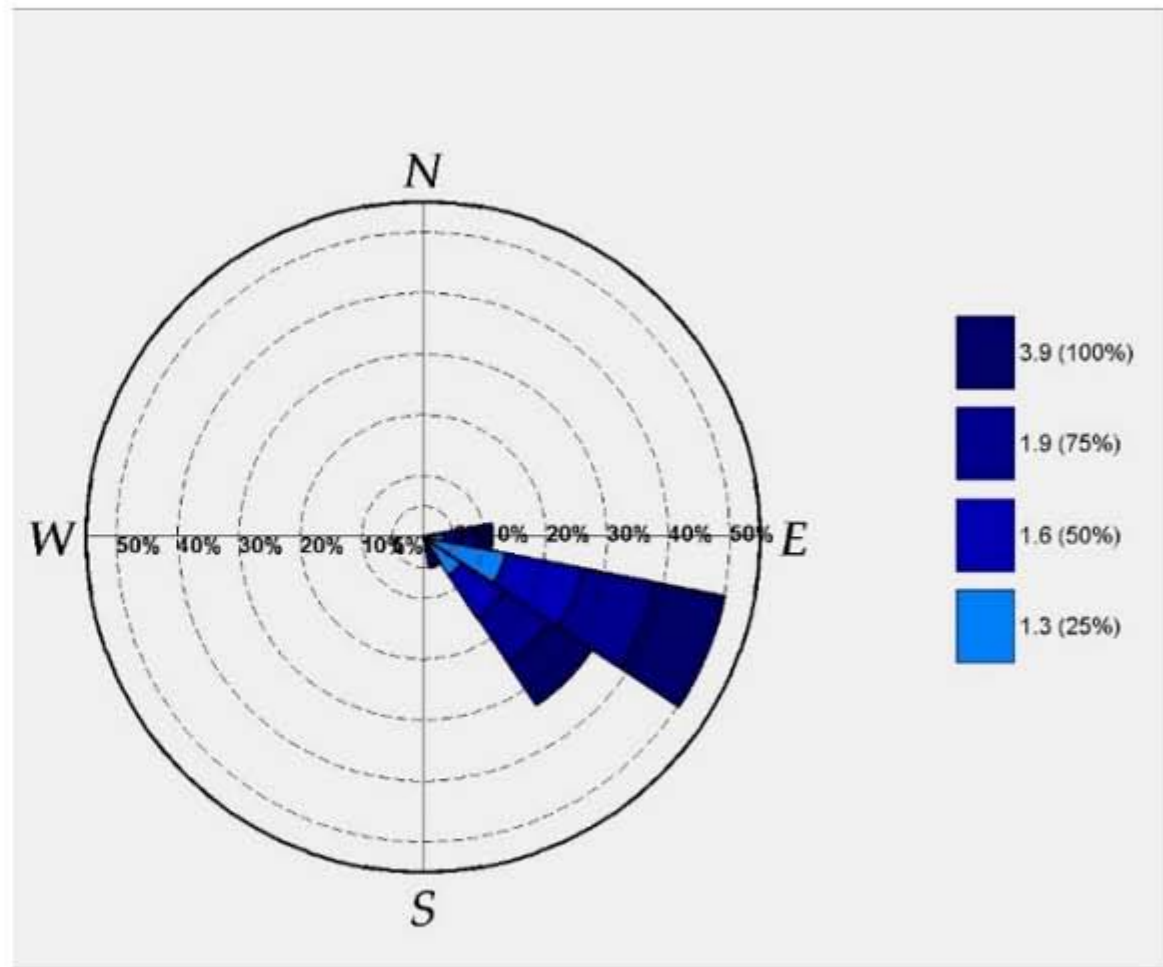
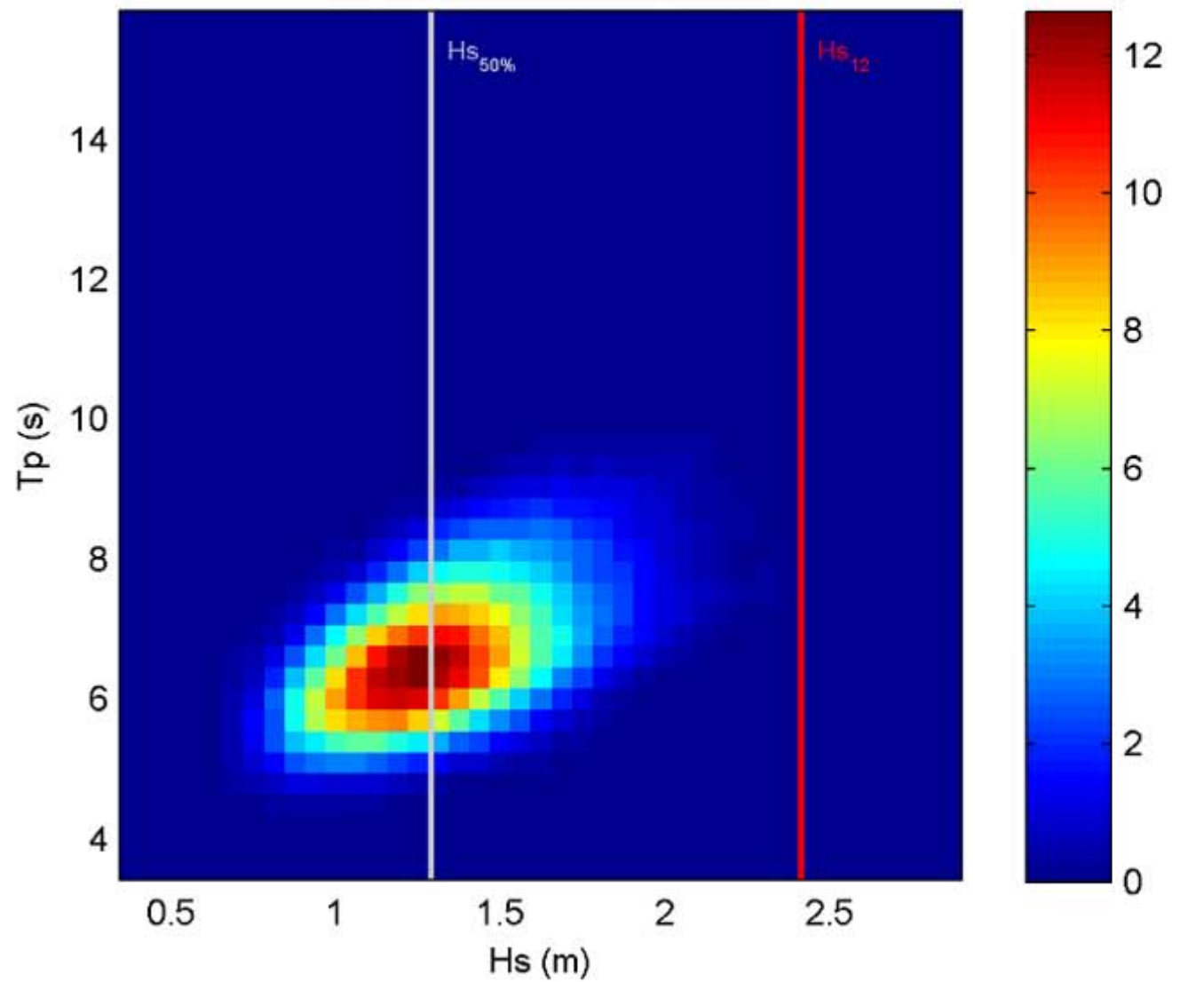
3 km

Ponta Grande, Bahia



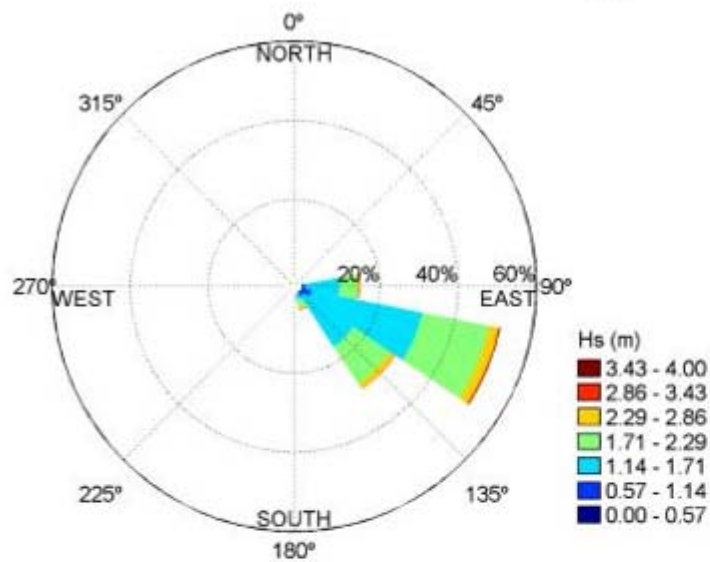


Hs – Tp density function



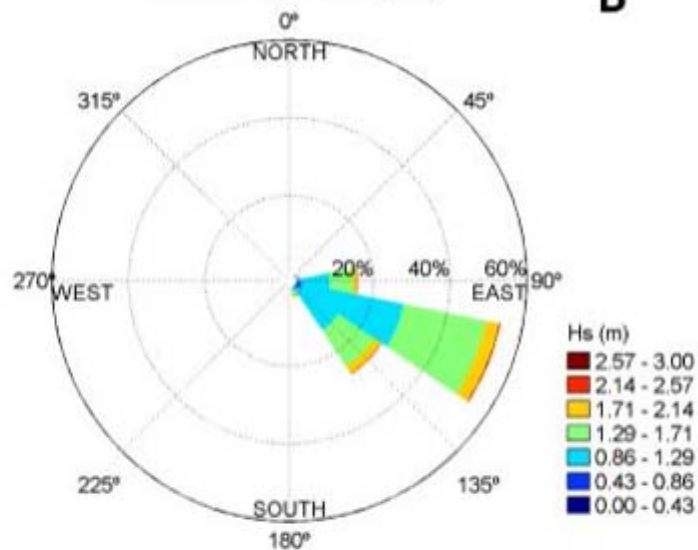
Directional *Hs* Rose (SON)

A



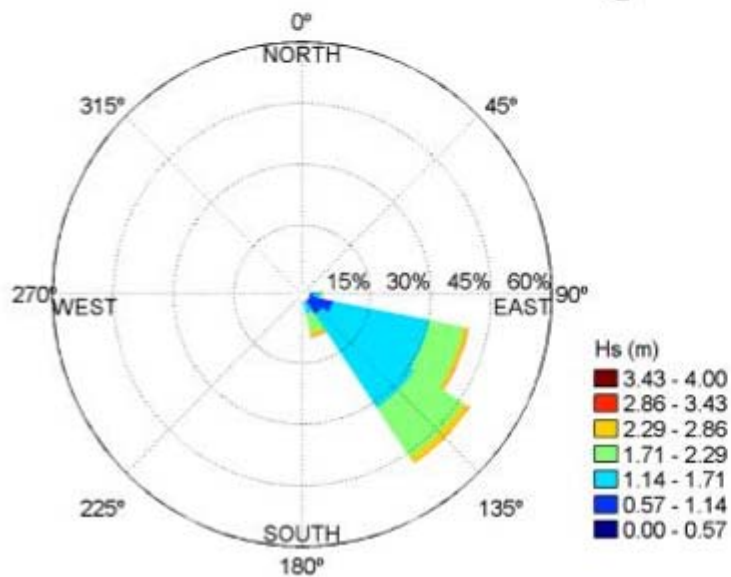
Directional *Hs* Rose (DJF)

B



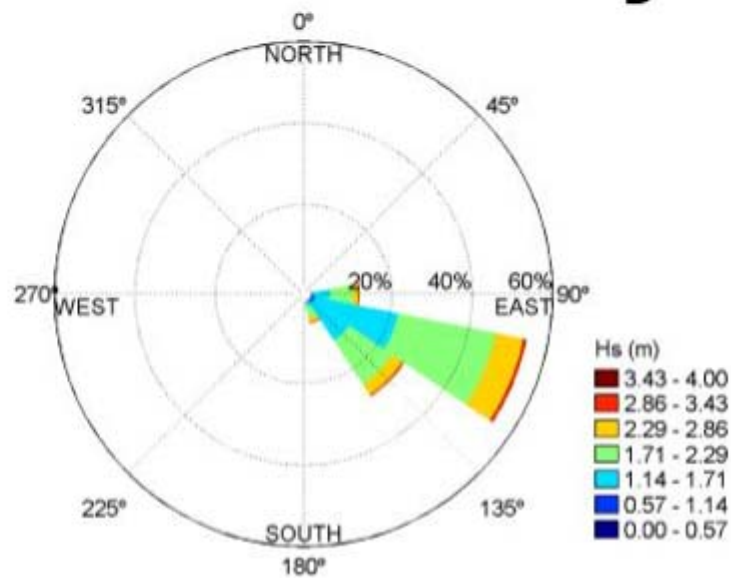
Directional *Hs* Rose (MAM)

C

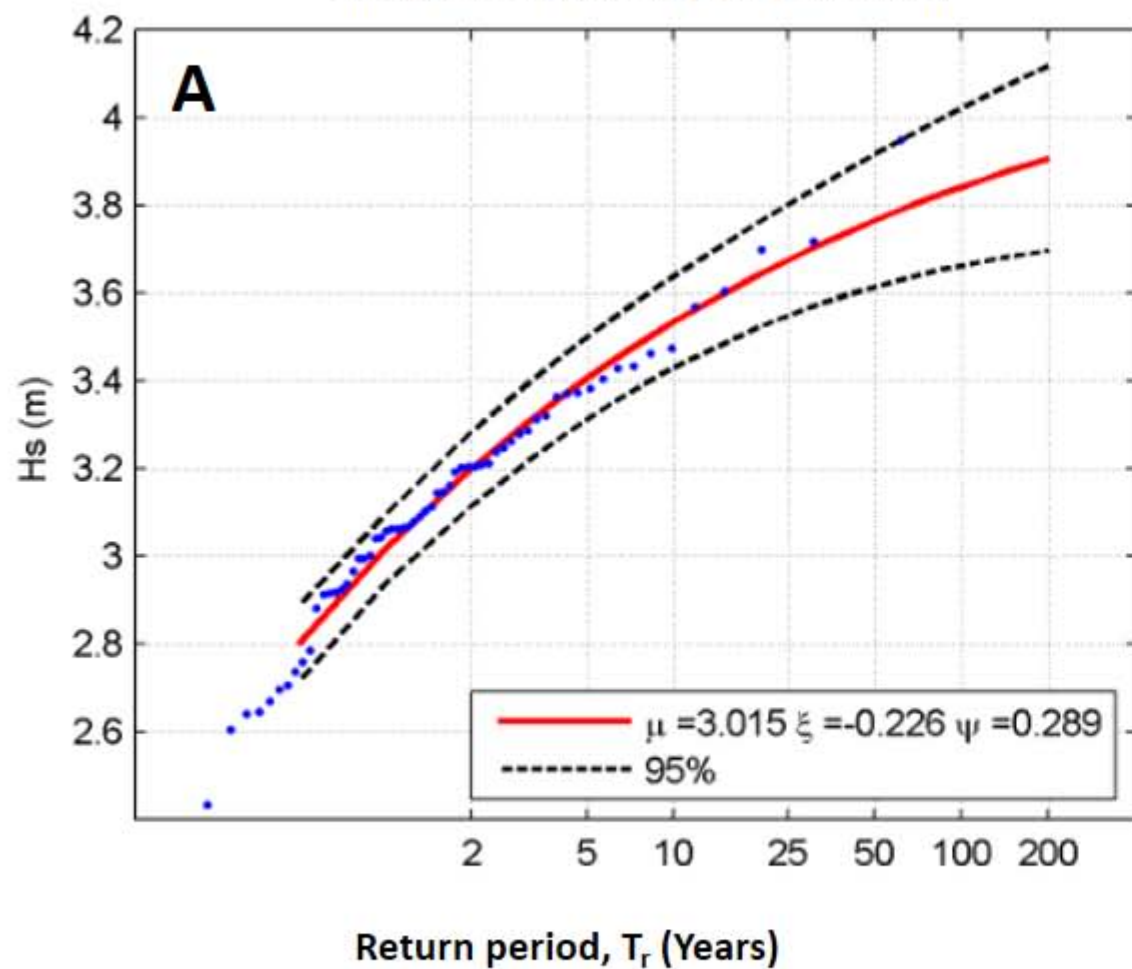


Directional *Hs* Rose (JJA)

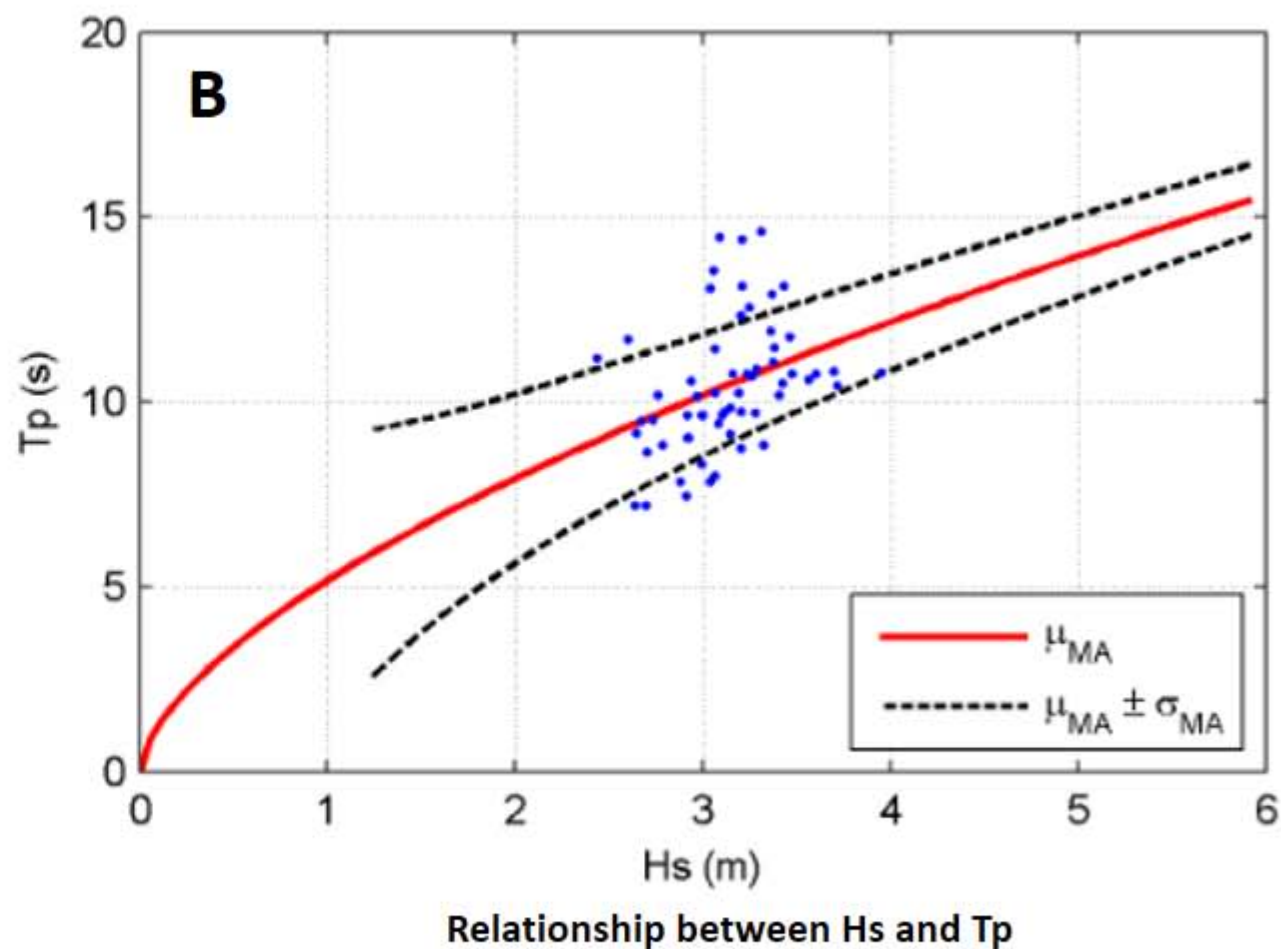
D



Extreme regimen adjusted by annual maximum values to a GEV function



Relationship between annual maximum values of H_s and T_p

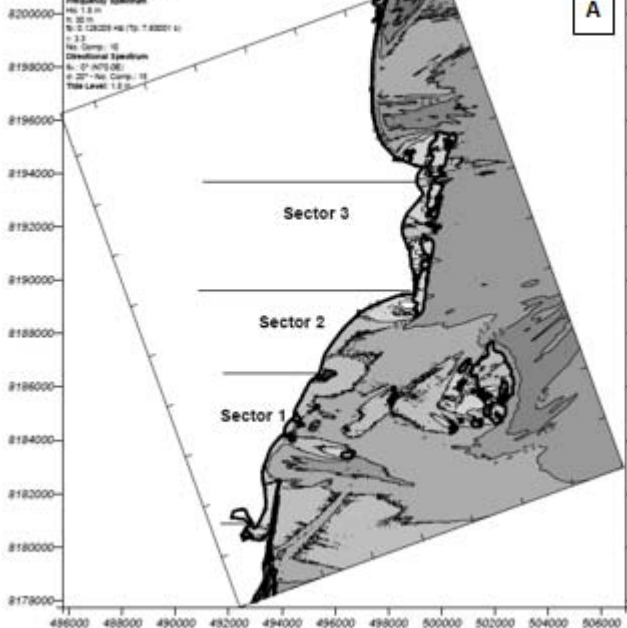


ENE WAVES

Frequency Spectrum

Hs: 1.8 m
T: 32 s
Tp: 3.128229 Hz (Tp: 7.432291 s)
N: 33
No Comp: 10
Directional Spectrum
N: 27°-N (75.0°)
P: 20°-No Comp: 10
Title Level: 1.8 m

A



SSE WAVES

Frequency Spectrum
Hs: 3 m
T: 25 m
T1: 5.12224 Hz (T2: 9.80228 s)
r: 7
No. Comp.: 10
Directional Spectrum
A: 27° (534.08)
C: 20° - No. Comp.: 10
Tide Level: 1.8 m

B

Sector 3

Sector 2

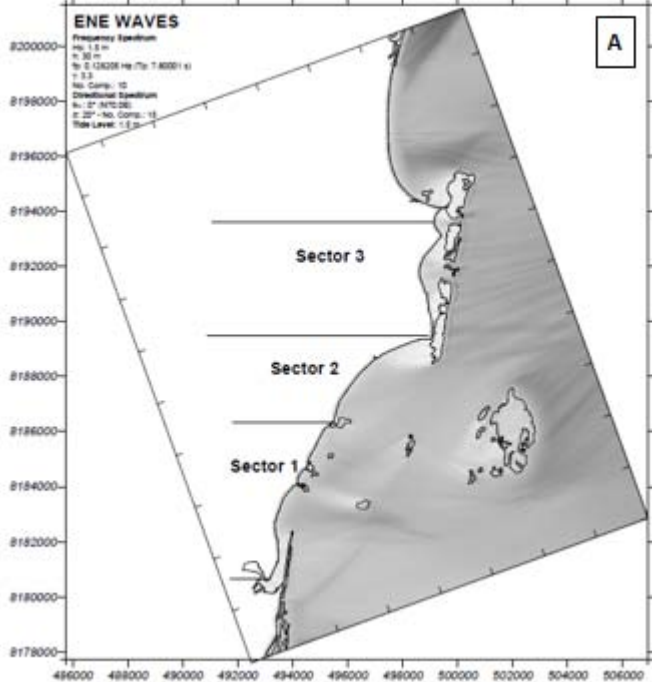
Sector 1



ENE WAVES

Frequency Spectrum
W: 1.5 m
T: 30 m
N: 0.12628 Hz (Tp: 7.80001 s)
T: 3.3
No. Comp.: 10
Directional Spectrum
W: 17° N10280
S: 20° - No. Comp.: 10
Tide Level: 1.5 m

A



SSE WAVES

B

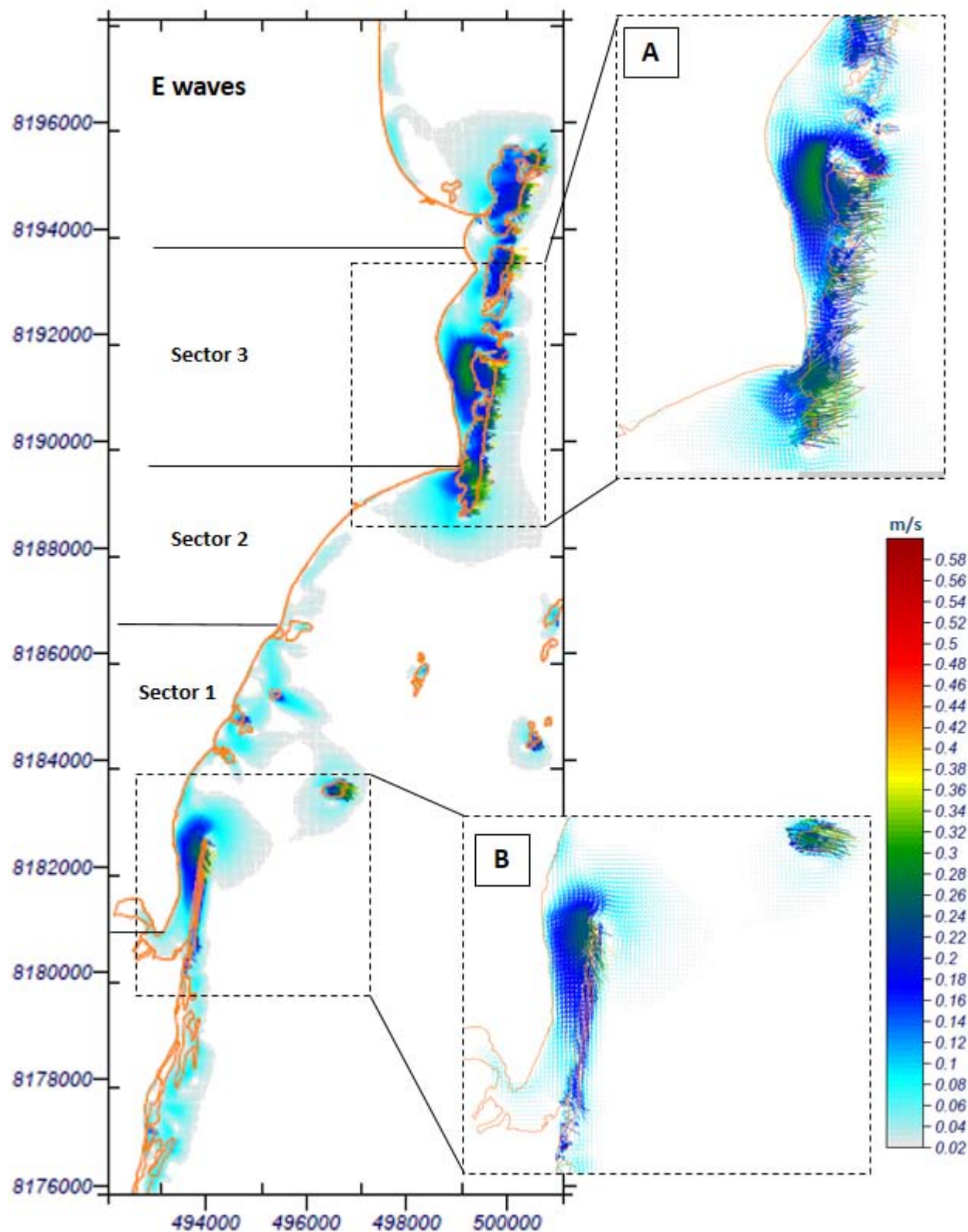
Frequency Spectrum
No. 3 m
No. 20 m
No. 0.10254 Hz (To: 9.89998 s)
N: 7
No. Comp.: 10
Directional Spectrum
No.: 0° (0.35.00)
or 20° - No. Comp.: 10
Tide Level: 1.5 m

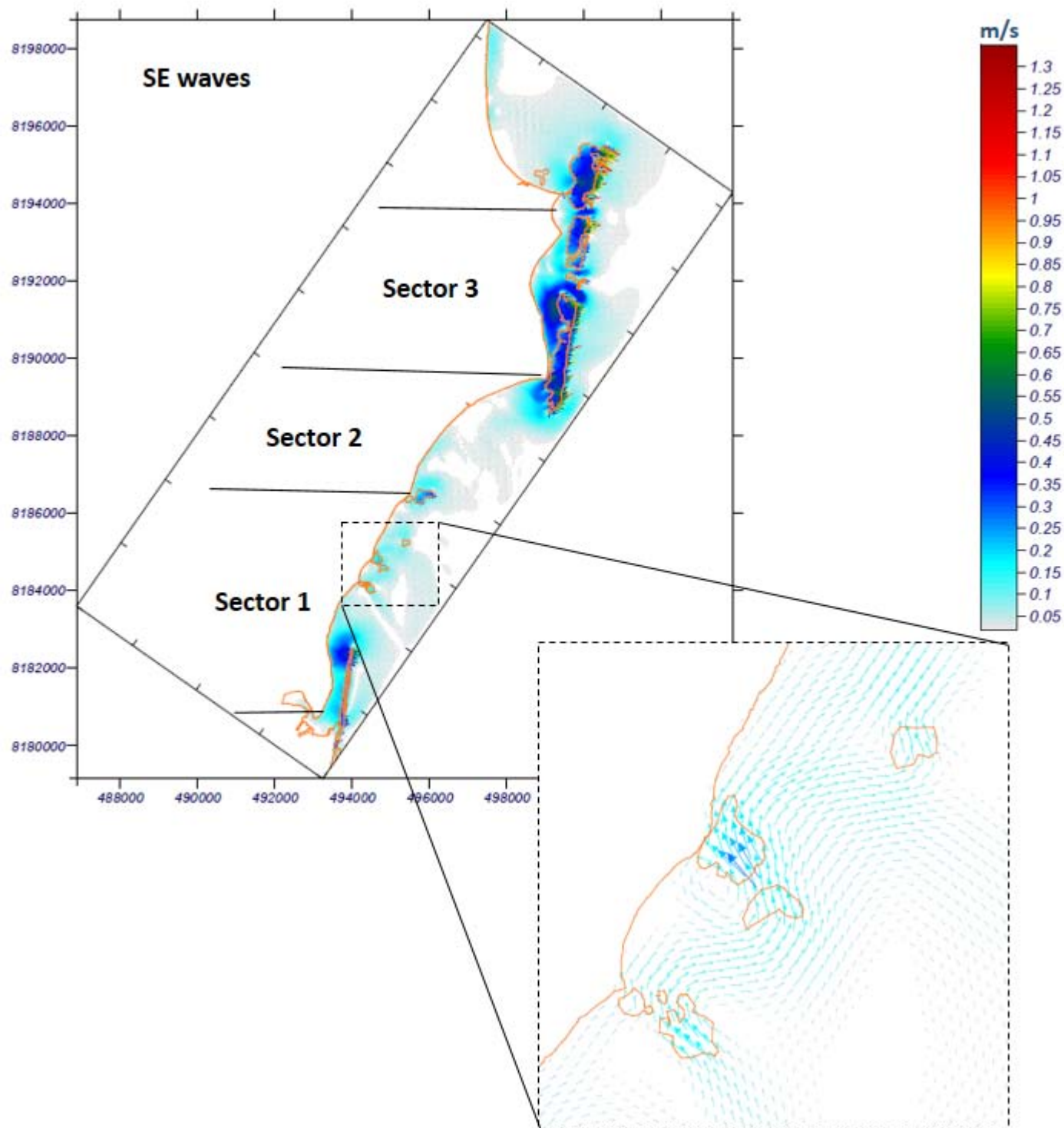
Sector 3

Sector 2

Sector 1







Direction	Occurrence probability (%)	Mean wave height (m)	More energetic wave height (m)	Mean wave period (s)	More energetic wave period (s)
ESE	50.08	1.53	3.17	7.45	12.32
SE	33.10	1.57	3.06	7.21	13.84
E	11.30	1.50	3.05	8.12	11.66
SSE	5.17	1.88	3.33	9.51	14.87